CryoLetters 23, 361-374 (2002)

The thermal effect of urethral warming during cryosurgery

Yoed Rabin* and Thomas F. Stahovich

Department of Mechanical Engineering
Carnegie Mellon University
Pittsburgh, PA 15213

Summary

The heating effect of urethral warming during cryosurgery has been investigated theoretically, via heat transfer simulations. Two warmer configurations have been considered: (i) the clinically available urethral warmer, which has a configuration of a counter flow fluid heat exchanger; (ii) a newly designed urethral warmer, based on a temperature controlled electrical heater, termed a "cryoheater". A dramatic effect of thermal resistance to heat transfer through the heat exchanger wall has been identified, which is absent in the cryoheater. It follows that the cryoheater is expected to be more efficient in generating an unfrozen region around the urethra. It is shown that the conventional heat exchanger may fail to prevent freezing around the urethra in a significant number of prostate cases, depending on the layout of cryoprobes around the urethra. On the other hand, clinical reports exist which suggest that the heat exchanger improves in many cases the outcome of cryosurgery, in terms of long term complications. It is speculated in the current report that the cryoheater can further improve the outcome of cryosurgery, by providing protection from freezing in a wider range of cases. It is suggested that a future study be conducted to examine the correlation between the layout of cryoprobes and surgical outcome.

Keywords: Cryosurgery, Cryoheater, Thermal Analysis, Prostate, Urethral Warmer

INTRODUCTION

Cryosurgery, which is the destruction of undesired biological tissues by freezing, has been a known surgical treatment since the middle of the 19th Century. Cryosurgery as an effective treatment of internal organs has been known since 1961, when Cooper and Lee presented the first cryosurgical device for treatment of internal tissues (7). The concept of cryosurgery as a minimally invasive procedure, using multiple cryoprobes, was developed in the mid 1980's as a consequence of remarkable developments in medical imaging, mainly in ultrasound and magnetic resonance imaging (MRI) (12-14,22).

Prostate cryosurgery was the first minimally invasive cryosurgical procedure to pass from the experimental stage and become a routine surgical treatment (14). The minimally invasive

* Email: rabin@cmu.edu ; Phone: (412) 268 2204 ; Fax: (412) 268 3348

approach created a new level of difficulty in cryosurgery, in which a well defined 3D shape of tissue must be treated, while preserving the surrounding tissues. To overcome this difficulty, a setup based on five minimally invasive cryoprobes was introduced during the early 1990's (2), followed by a six cryoprobe setup in the late 1990's (Erbe Elektromedizin GmbH, Germany), all based on liquid nitrogen cooling. With recent technological developments in Joule-Thomson cooling, the diameter of the cryoprobe has been dramatically decreased, and the number of cryoprobes increased (Endocare, Inc., CA; Galil-Medical, Inc., Israel).

With the dramatic increase in the number of cryoprobes, a new challenge has been introduced to cryosurgery, that is, how to shape the frozen region and limit the destructive freezing effect to the target area. A good example of a device that prevents freezing is the so-called "urethral warmer", which is used routinely in prostate cryosurgery. Technically, the urethral warmer is a double-pipe water heat exchanger, embodied in a standard catheter. Water, from a reservoir at close to normal body temperatures, is pumped through the catheter, to maintain the urethra temperature above freezing. The double-pipe heat exchanger configuration means that the fluid flows through an internal tube towards the tip of the catheter, and flows back through a coaxial external tube. The urethral warmer has proven to reduce post cryosurgery complications associated with damage to the urethra in many cases (6). This heat exchanger is the only warmer available today for routine cryosurgery control.

A new means of cryosurgery control has been suggested recently, based on a minimally invasive electrical heater, which is termed a "cryoheater" (18). One potential use of the cryoheater is temperature control of the 3D shape of the frozen region (21). Another possible application is similar to the available urethral warmer (6), where the heat exchanger mechanism at the tip of the catheter is replaced with a temperature controlled electrical heater (18). To the best of our knowledge, the electrical heater application for urethral warming has never before been tested clinically.

One of the most common questions raised in discussions related to the application of the urethral warmer is "what is the extent of freezing prevention achieved by the urethral warmer?" (19). The purpose of this study is twofold: (i) to analyze the potential heating effect of the urethral warmer as a freezing prevention mechanism, and (ii) to study the potential effect of the cryoheater as a substitute for the available urethral warmer. The current study is based on computer simulations of bioheat transfer.

To avoid confusion in terminology between the different technologies, we refer to both the available heat exchanger urethral warmer, and the recently presented cryoheater, as "urethral warmers". However, the available warmer is also referred to as a "heat exchanger", while the new heating technology is also referred to as a "cryoheater", where deemed appropriate.

CRYOHEATER SETUP

A feasibility study of the cryoheater application in a gelatin solution has been presented recently (21). For the purpose of clarification, this new technology is presented here briefly.

A schematic illustration of the cryoheater setup as a urethral warmer is shown in Fig. 1. The heating element is an electrical resistor, encapsulated in a metallic cylinder, located at the tip of a urethral catheter. The metallic cylinder has the same outer diameter as the catheter. A temperature sensor is connected to the inner wall of the metallic cylinder, midway between the ends of the electrical heater. The difference between the cryoheater presented by Rabin and Stahovich (21) and the cryoheater presented in the current study, is that the former has an external shape similar to a cryoprobe, while the latter has an external shape similar to a urethral catheter, as discussed in more detail by Rabin et. al. (18). However, the technique of heating and temperature control is similar in both cryoheater applications.

The cryoheater is connected to a temperature controller with two connectors, one for the temperature sensor (which is used as feedback for the temperature control mechanism), and one for powering the electrical resistor. The temperature controller is connected to a power supply, which supplies electrical power to the heater. The cryoheater is activated prior to initiation of freezing with a temperature set point of 37°C, which remains constant through the cryoprocedure.

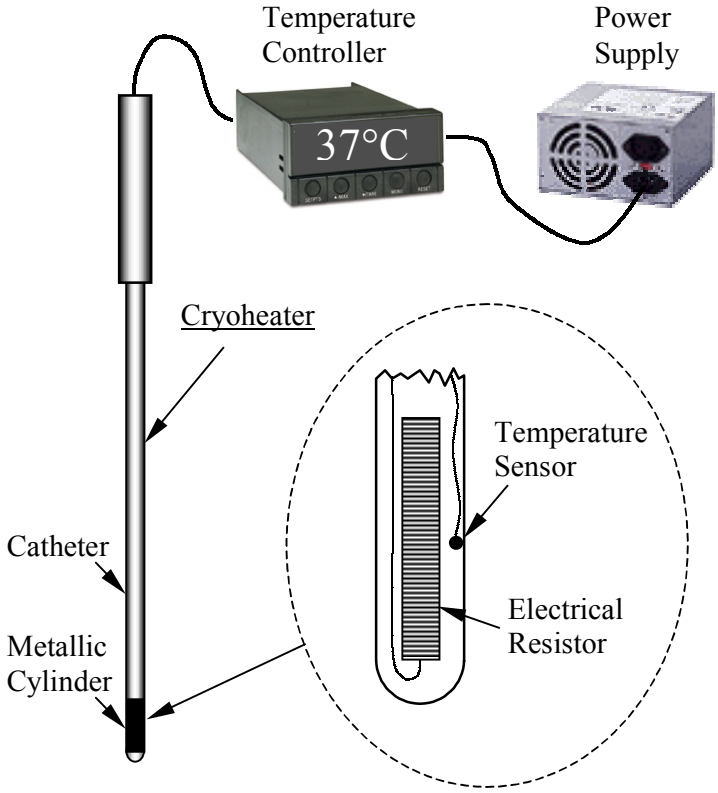

Figure 1: Schematic illustration of the cryoheater setup. The cryoheater has the same external configuration as a standard urethral warmer, which is similar to a urethral catheter.

MATHEMATICAL FORMULATION

In order to analyze the heating effect of the urethral warmer -- whether a heat exchanger or a cryoheater -- two numerical simulation codes have been written. One code examines a transient freezing process, while the other code examines an advanced stage of cryosurgery, when heat transfer approaches a steady state. The rationale in analyzing these two cases is addressed below.

It is customary to assume that heat transfer in the presence of blood perfusion can be modeled by the classical bioheat equation (15):

$$C\frac{\partial T}{\partial t} = \nabla \cdot (k\nabla T) + w_b C_b (T_b - T) + q_{met} \tag{1}$$

where C is the volumetric specific heat of the tissue, T is the temperature, t is the time, k is the thermal conductivity of the tissue, w_b is the blood perfusion rate (measured in volumetric blood flow rate per unit volume of tissue), C_b is the volumetric specific heat of the blood, T_b is the blood temperature entering the thermally treated area (typically the normal body temperature), and q_{met} is the metabolic heat generation. Note that for blood perfusion, the product of w_bC_b is typically cited in the biothermal literature.

Numerous scientific reports have been published questioning the mathematical consistency of the above classical bioheat equation, and its validity, while suggesting various alternatives (5,11,23,24). Overviews and discussions regarding these models have been presented by Charny (3) and Diller (8). In broad terms, the classical bioheat equation is commonly assumed to be suitable for representing heat flow in the presence of a dense capillary network, and not in the presence of major blood vessels. In fact, the blood perfusion rate is often found by regression of experimental data to theoretical predictions, based on the classical bioheat equation (16). It is assumed here that a more advanced model of bioheat transfer will not guarantee greater accuracy in the cryosurgery simulation, but it will involve greater mathematical complications, and it is deemed unnecessary for the purpose of the current study. Note that metabolic heat generation is typically negligible compared to the heating effect of blood perfusion and is neglected in this study (9). However, for consistency in presentation, this term will also appear in the numerical formulation of the bioheat equation.

The numerical scheme applied to the transient problem has been presented by Rabin and Shitzer (17), and is presented here briefly. This numerical scheme is based on a finite difference formulation of Eq. (1), which, after rearrangement, becomes:

$$T_{i,j,k}^{p+1} = \frac{\Delta t}{\Delta V_{i,j,k}[C_{i,j,k} + (w_b C_b)_{i,j,k}\Delta t]} \sum_{l,m,n} \frac{T_{l,m,n}^{p} - T_{i,j,k}^{p}}{R_{l,m,n\text{-}i,j,k}} + \frac{\Delta t[(w_b C_b)_{i,j,k} T_b + (q_{met})_{i,j,k}] + C_{i,j,k} T_{i,j,k}^{p}}{C_{i,j,k} + (w_b C_b)_{i,j,k}\Delta t} \tag{2}$$

where i,j,k and l,m,n are space indexes, p is a time index, ΔV is an element unit volume, Δt is a time interval, and R is a thermal resistance to heat transfer between node i,j,k and its neighbor l,m,n. In a Cartesian geometry, the typical thermal resistance in the x direction is:

$$R_{l,m,n\text{-}i,j,k} = \frac{\Delta x_{l,m,n}}{2k_{l,m,n}\Delta y_{l,m,n}\Delta z_{l,m,n}} + \frac{\Delta x_{i,j,k}}{2k_{i,j,k}\Delta y_{i,j,k}\Delta z_{i,j,k}} \tag{3}$$

where x,y,z are coordinates (17). The bioheat transfer problem is solved in an infinite domain from the perspective of heat transfer. The infinite domain is simulated by a finite domain with an infinite resistance at the outer boundary. In practice, a radius of 50 mm was found large enough to be considered infinite, i.e., a radius beyond which the initial temperature remains unchanged during the simulated process of freezing. Equation (2) is solved explicitly for every numerical grid point, and is conditionally stable. Incorporation of phase change in the scheme is based on the enthalpy approach, where the latent heat effect is taken into account via an effective specific heat property within the phase transition temperature range. Detailed discussion regarding the stability criteria and the applicability of the current numerical

scheme to cryosurgery has been presented by Rabin and Shitzer (17).

The input for the solution presented in Eq. (2) includes: the cryoprobe and urethral warmer temperature protocols, the initial temperature of the biological tissue, dimensions, and typical physical properties of biological tissues (Table 1). The outputs are the temperature distribution and the location of the freezing front, where the latter is interpolated from the prior.

One possible technique for solving the steady state case is to run the transient solution, Eq. (2), until a steady state has been reached. However, due to the stability criterion associated with this numerical scheme, which leads to very small time intervals, the transient approach as a means of generating a steady state solution is very expensive. Since the current study includes an intensive parametric study, in which the numerical solution is repeated extensively, the approach of generating a steady state solution by going through the entire transient process was abandoned.

At steady state, the left side term of Eq. (1) becomes zero, which can lead to the following numerical scheme:

$$0 = \sum_{l,m,n} \frac{T_{l,m,n} - T_{i,j,k}}{R_{l,m,n-i,j,k}} + (w_b C_b)_{i,j,k}(T_b - T_{i,j,k}) + (q_{met})_{i,j,k} \tag{4}$$

where the time level index p, previously presented in Eq. (2), has no meaning at steady state. As before, the metabolic heat generation term is given here only for consistency in presentation with the classical bioheat equation.

Equation (4) is solved simultaneously for all grid points, using an iterative predictor-corrector technique, as follows: (i) The temperature distribution at steady state is predicted (first prediction is arbitrary, and can be taken as normal body temperature). (ii) All thermal resistances to heat transfer, $R_{l,m,n-i,j,k}$, are calculated for the predicted temperature distribution. (iii) An improved temperature distribution at steady state is calculated for each numerical grid point by satisfying Eq. (4) for all numerical grid points simultaneously; this is the correction of the temperature distribution. If the predicted temperature distribution is found to be insignificantly different from the corrected distribution, the corrected temperature distribution becomes the final solution. However if the latter difference is found to be significant, the corrected temperature distribution is used as the next prediction, and stages (ii)-(iii) are repeated, until the process of prediction-correction converges. It can be shown mathematically that this process will always converge to a unique solution. A temperature difference of less than 10^{-4} °C was deemed appropriate as a threshold for convergence in the current study. It is interesting to note that, typically, 10 to 20 prediction-correction cycles were required to reach a steady state solution, while 10^6 cycles were typically required to take a transient solution to a steady state, through the simulation of the entire cryosurgical process. Note that during this process, the thermal conductivity value may vary by a factor of 5 in the relevant cryogenic temperature range, which slows the process of convergence for the steady state solution.

MATHEMATICAL MODEL

In order to answer the question “what is the extent of freezing prevention achieved by the urethral warmer?”, a worst case scenario was chosen, that being steady state in a 2D geometry. The term “worst case” refers to the smallest region around the urethra, which is protected from the destructive effect of freezing. The steady state represents a worst case scenario in the time domain, after the moderating effect of latent heat absorption has

disappeared. The 2D represents a worst case scenario in space, since it actually represents an infinitely long warmer, cooled by infinitely long cryoprobes. In reality, axial heat conduction to the cryoprobes and the warmer prevails, which decreases the cooling capabilities of the cryoprobes, but increases the heating capabilities of the urethral warmer. It follows that less heat is likely to be drawn from the urethral warmer by the cryoprobes in the 3D case.

The number of possible prostate geometries and cryoprobes setups is virtually endless. Six cryoprobes were used in earlier cryosurgery devices. Although the possible number of simultaneously applied cryoprobes has increased with the years, six is a practical limit for the number of cryoprobes to be localized on a single plane. Therefore, a six cryoprobe setup has been chosen for the purpose of the current study, as illustrated in the insets in Figs. 2-4. For simplicity, we further assume that the cryoprobes are uniformly distributed circumferentially, at a fixed radius from the urethral warmer center. The radial location of these cryoprobes is the studied parameter, since it is directly related to the thickness of the region affected by the urethral warmer. The possible effect of an uneven distribution of cryoprobes on a single plane has been recently presented by Rabin and Stahovich (21).

Table 1 lists typical values of thermophysical properties of biological tissues, which were used in the current study. For the purpose of this study, biological tissues are assumed to have a phase transition temperature range between 251K and 273K (similar to NaCl solution). The specific heat within the phase transition temperature range is an effective property, which includes the latent heat effect (17). Maximal possible blood perfusion was assumed in all cases but one, generating a heating effect of w_bC_b=40 kW/m^3-°C. The single exception was used to demonstrate the effect of a lower blood perfusion rate on the results of this study, as discussed in the steady state analysis section.

Table 1: Representative thermophysical properties of water and soft biological tissues used in the current analysis (T in degree K) (1,4,20)

Property	Water		Soft Biological Tissues	
Thermal conductivity, k, W/m-K	0.6 $2135\times T^{-1.235}$	273<T T<273	0.5 $15.98-0.0567\times T$ $1005\times T^{-1.15}$	273<T 251<T<273 T<251
Volumetric specific heat, C, kJ/m^3-K	4180 $4.14\times T$	273<T T<273	3600 15,440 $7.57\times T$	273<T 251<T<273 T<251
Latent heat, L, MJ/m^3	330		300	
Blood perfusion heating effect, w_bC_b, kW/m^3-K	0		0-40	

Analysis of the Transient Freezing Process

The analysis of the transient freezing process is focused on the cryoheater, while the analysis of steady state includes a comparison of the heat exchanger with the cryoheater, as discussed in the next section. In the analysis of the transient process, the following working conditions are assumed: (i) a constant cryoheater set point of 37°C; (ii) the cryoprobe is cooled at a constant cooling rate from the initial temperature of 37°C to -145°C in 30 sec.,

followed by a constant cryoprobe temperature of -145°C (21). A cryoprobe diameter of 1.5 mm, and a warmer diameter of 5 mm, were also assumed.

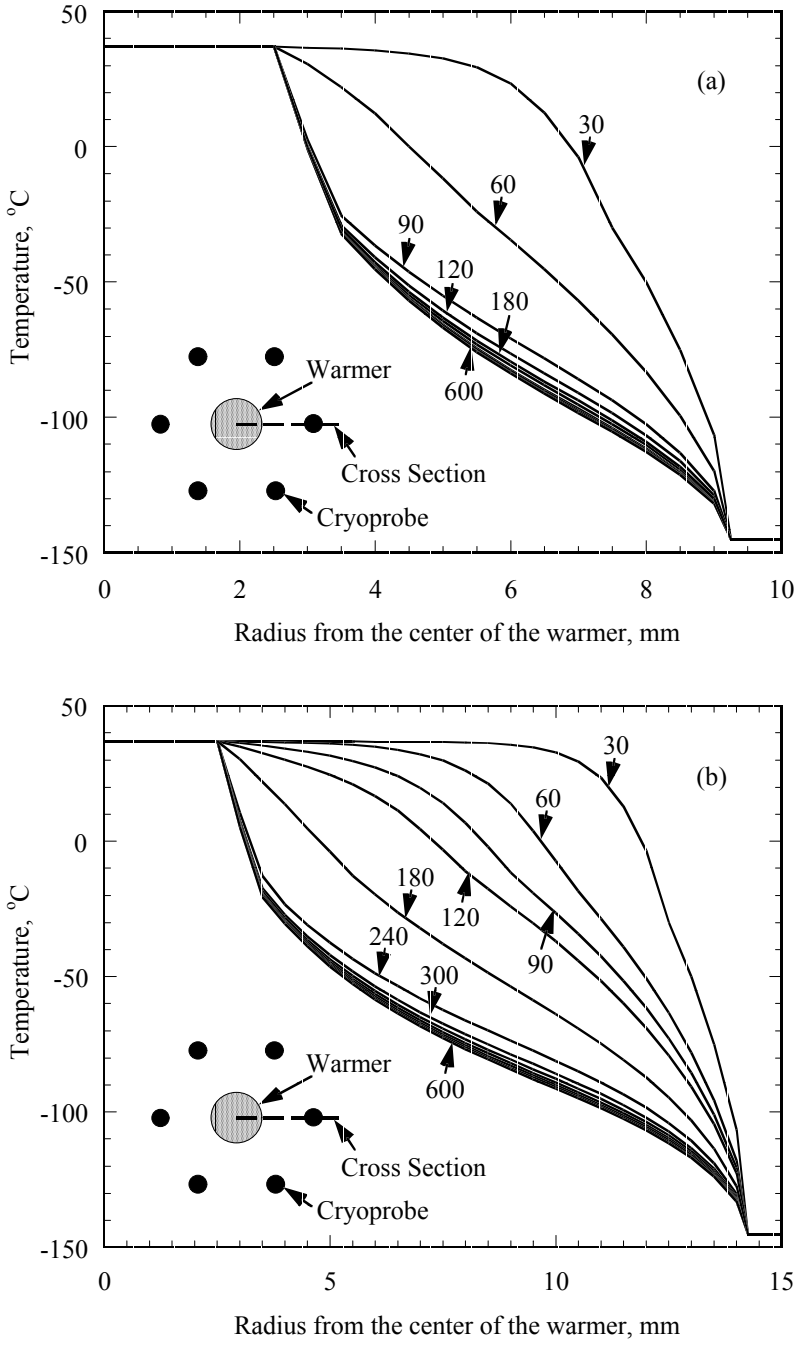

Figure 2: Radial temperature distribution measured from the center of the urethral warmer, for the 2D case of a cryoheater and 6 cryoprobes. The cryoprobes are evenly distributed circumferentially, at a radius of: (a) 10 mm, and (b) 15 mm. The temperature distribution is given between the warmer and a representative cryoprobe, along a cross section represented by the dashed line in the inset. Temperature distributions are given every 30 sec. for the first 120 sec., and every 60 sec. thereafter.

The radial temperature distribution is shown in Fig. 2, for a distance between the center of the warmer and the center of the cryoprobe of: (a) 10 mm, and (b) 15 mm. It can be seen from Fig. 2(a) that the temperature distribution between the cryoheater and the cryoprobe reaches steady state during the typical duration of a cryosurgery procedure, where the duration of freezing is typically measured in minutes. For example, the maximum temperature difference between the temperature distribution at 120 sec. and at 180 sec. is about 3.5°C, while the same difference between 240 sec. and 600 sec. is also about 3.5°C. The maximal change in temperature over time after 600 sec. is less than 10^{-2} °C per 60 sec. In fact, for all practical cases, steady state can be assumed after 480 sec. (4 minutes).

Similar observations can be made from Fig. 2(b), however the steady state is approached somewhat slower, due to the greater distance between the cryoprobes and the cryoheater. A third case has also been analyzed, in which the cryoprobes are located at a radial distance of 5 mm from the urethral warmer, but the resulting temperature distribution in this case could already be considered steady state after 30 sec., and a graphical presentation of these results was deemed uninformative.

It can be seen from Fig. 2 that, in general, the lowest values of the temperature distribution are found at steady state. This observation supports the underlying assumption that the steady state case is the worst case scenario in the time domain.

The discussion regarding transient versus steady state has thus far focused on the region between the urethral warmer and the cryoprobes (inner region). Figure 3 presents the radial temperature distribution for the same case presented in Fig. 2(b), but for the region outside the circle of cryoprobes (outer region). It can be seen that for a typical duration of freezing, no steady state may be assumed in the outer region.

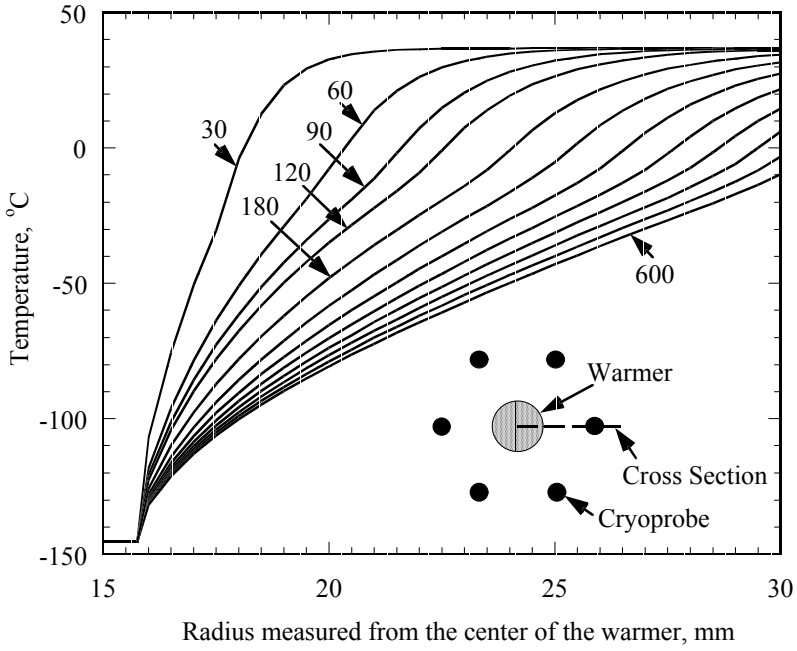

Figure 3: Radial temperature distribution measured from the center of the urethral warmer, for the 2D case of a cryoheater and 6 cryoprobes. The cryoprobes are evenly distributed circumferentially, at a radius of 15 mm. The temperature distribution is given from a representative cryoprobe outwards, along a cross section represented by the dashed line in the inset. Temperature distributions are given every 30 sec. for the first 120 sec., and every 60 sec. thereafter.

Analysis of the Steady State

It has been shown in this report that the temperature distribution in the inner region is likely to reach steady state during a typical cryoprocedure. Since the inner region is the region of interest for the analysis of heating by the urethral warmer -- and in order to save computational efforts -- the analysis is now focused on the steady state.

Two typical cases are now considered. Case I is a cryoheater with an external diameter of 5 mm, and a temperature of 37°C on its outer surface. Case II is a heat exchanger with an external diameter of 5 mm, and wall thickness of 0.5 mm. It is assumed that the water flowing through the heat exchanger is well mixed, and that the flow rate is high enough, so that a temperature of 37°C is achieved at the inner surface of the tube. These conditions represent optimal performance of a heat exchanger. Actual performance would be less due to a down stream decrease in fluid temperature, and due to a temperature gradient in the flow cross section. The tube is composed of polymeric material (tygon, for example), having a typical thermal conductivity of 0.2 W/m-°C.

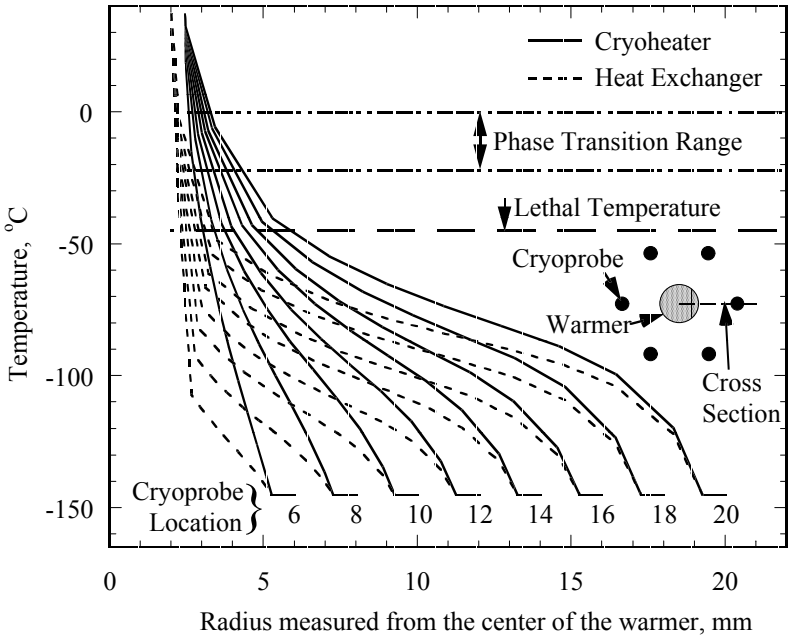

Figure 4: Radial temperature distribution at steady state for various cryoprobe locations. External diameter of both heat exchanger and cryoheater is 5 mm. Wall thickness of the heat exchanger is 0.5 mm. A boundary condition of 37°C is imposed on the heat exchanger internal wall, and on the cryoheater external surface.

Figure 4 presents the temperature distribution for a series of cryoprobe locations, for both cases I and II. Note that the temperature distribution starts at the inner wall for case II. The dramatic effect of thermal resistance to heat transfer through the heat exchanger wall can be clearly seen from Fig. 4, where tissue temperature in the vicinity of the cryoheater is significantly higher. For convenience, three temperature levels are also shown in Fig. 4: the upper boundary of phase transition, 0°C, the lower boundary of phase transition, -22°C, and the so-called lethal temperature of -45°C. The term "lethal temperature" is defined as a temperature threshold below which maximum cryodestruction is achieved. A review of

possible values for the lethal temperature is given by Gage and Baust (10), and the value of -45°C is chosen for illustration purposes only, bypassing the discussion about the actual value of this threshold. Figure 5 presents the location of the above three isotherms, for both cases I and II. In case II for example (heat exchanger), the distance of the lethal temperature (-45°C) isotherm from the warmer is zero for cryoprobe locations of less than 11 mm. This means that the outer temperature of the heat exchanger is below -45°C, which results in no thermal protection of the urethra wall. At a cryoprobe location of 11 mm, the lethal temperature distance in case I (cryoheater) is about 1.3 mm away from the warmer's wall, which covers the entire urethra wall (the urethra wall is measured in tenths of a millimeter).

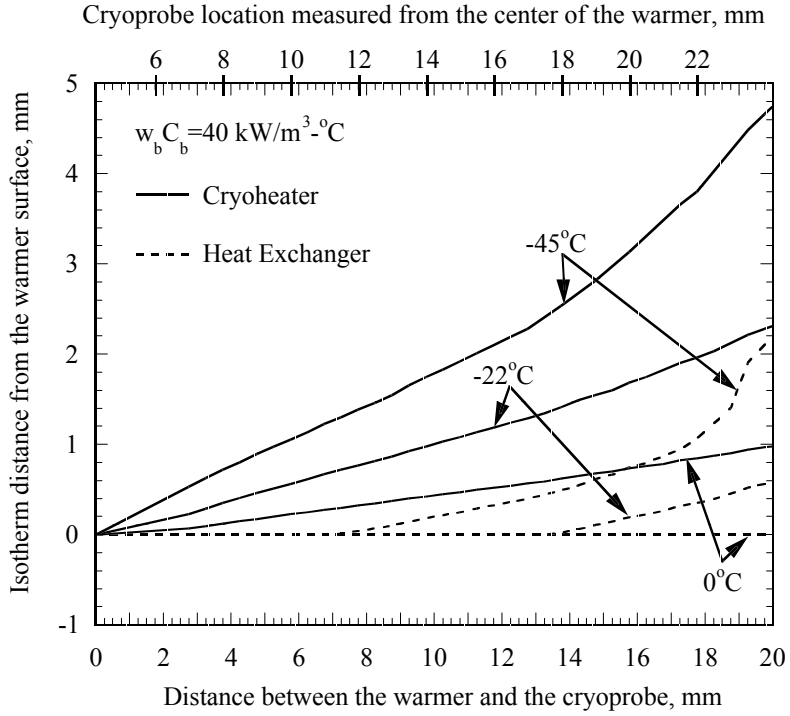

Figure 5: Location of isotherms as a function of the locations of cryoprobes, at steady state, for a heat exchanger (case I) and a cryoheater (case II).

In general, it can be seen that the heating effect of the urethral warmer is highly dependent on the location of the cryoprobes, regardless of the heating technique. The possible protection effect is measured, at most, in a few mm. However, there is a significant range of radial locations of the cryoprobes in which the heat exchanger is predicted to be inadequate to prevent the cryodestruction effect.

The heat exchanger has a significant thermal resistance to heat conduction through its tube wall, while the cryoheater has none, which makes the cryoheater superior in terms of the maximum radius protected from freezing. Obviously, the circulated water temperature could be set higher, to compensate for the dramatic decrease in temperature across the heat exchanger wall. However, the required elevation in temperature is related to the specific radial location of the cryoprobes. Clinical verification of the actual cryoprobe location is associated with an extremely high level of uncertainty. If the temperature set point for the heat exchanger is over estimated, hyperthermia damage to the urethra may take place. It is further emphasized that this ideal distribution of six cryoprobes is made in order to simplify the current thermal

analysis. In the case of a heat exchanger in a real cryosurgery procedure, the distance between the different cryoprobes and the warmer varies, which may cause insufficient heating along only some circumferential regions of the urethral warmer. Such partial circumferential heating is unlikely to occur in the case of a cryoheater, due to the high thermal conductivity of the cryoheater (a metallic cylinder), which is two to three orders of magnitude higher than the thermal conductivity of the tissue.

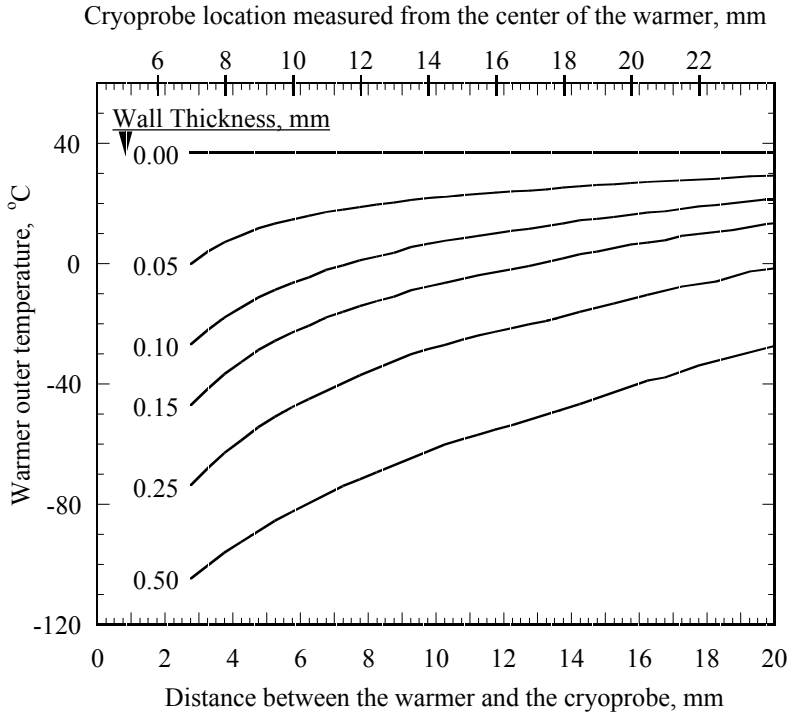

Figure 6: Outer heat exchanger temperature as a function of the cryoprobes location for various thickness' of the heat exchanger wall.

It is evident that the thickness of the wall of the heat exchanger has a major effect on its thermal performance. Figure 6 presents a parametric study of the effect of the heat exchanger wall thickness on its outer temperature. The circumferential temperature variation on the outer surface of the heat exchanger was found to be less than 2°C for all studied cases, and its minimum value is shown in Fig. 6. In Fig. 6, zero thickness practically represents the cryoheater. It can be seen from Fig. 6 that a very thin wall thickness of 0.05 mm is required in order to maintain the outer temperature of the heat exchanger above freezing within the entire range of cryoprobe locations studied for this report. A wall thickness of 0.05 mm of a polymeric tube is extremely thin, and is not likely to sustain the pressure required to force water through the heat exchanger.

Finally, the maximum possible blood perfusion rate has been assumed for the case studies presented above. In order to test the thermal effect of this assumption, simulations were repeated for lower blood perfusion rates, and the results of various blood perfusion rates have been compared. For example, Fig. 7 shows the location of isotherms in the cryoheater case for two rates of blood perfusion: (i) maximum, producing a heating effect of 40 kW/m^3-°C (also shown in Fig. 5); and, (ii) one half of the maximal blood flow rate, producing a heating effect of 20 kW/m^3-°C. It can be seen from Fig. 7 that the heating effect of blood perfusion within the inner region is minor. This should not be surprising since most of the inner region is

frozen, with no blood supply. On the other hand, the blood perfusion rate may have a significant effect on the simulated temperature distribution in the external region, where the overall size of the frozen region is affected by blood perfusion. Note that a steady state is achieved when the overall heating effect of blood perfusion reaches an energy balance with the overall cooling effect of the cryoprobes, minus the heating effect of the warmer. It follows that results presented in previous figures, with regard to the inner region, are not sensitive to the rate of blood perfusion. Rabin and Shitzer (17) offered further insight into the heating effect of blood perfusion in the transient process, and its relation to the rate of growth of the frozen region.

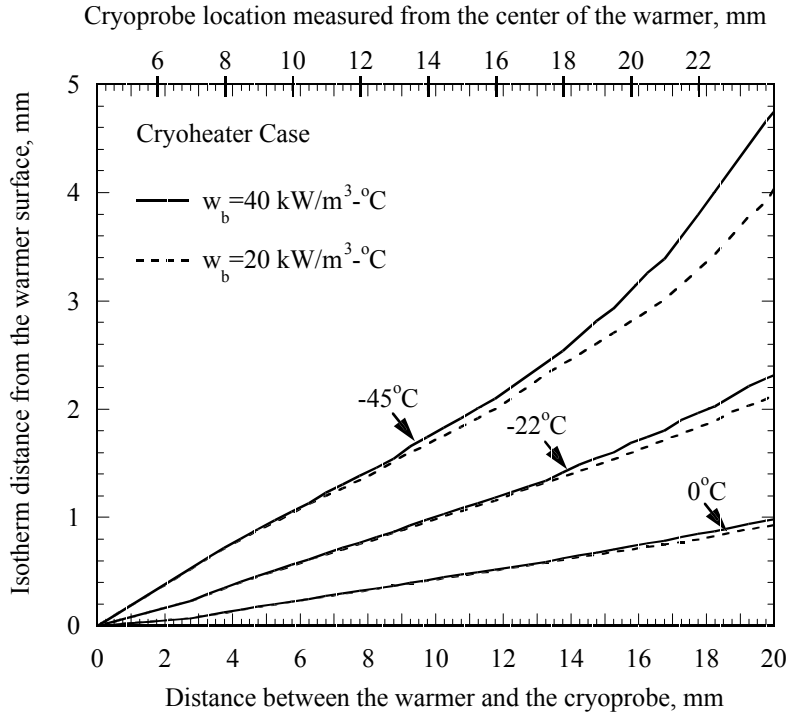

Figure 7: Location of isotherms as a function of the locations of cryoprobes, at steady state, for the case of a cryoheater (case II), and for two cases of blood perfusion rate. The value of 40 kW/m^3-°C is associated with maximum possible blood perfusion.

SUMMARY AND CONCLUSIONS

The heating effect of the urethral warmer has been investigated theoretically via bioheat transfer simulations. Two warmers have been considered: (i) the clinically available urethral warmer, which has the configuration of a double-pipe counter flow heat exchange, and (ii) a recently developed urethral warmer, which has the configuration of a temperature controlled electrical heater, termed a "cryoheater".

For the purpose of this study, a simplified mathematical problem has been considered, combining 6 cryoprobes at a fixed distance around a urethral warmer, which are evenly distributed circumferentially. The radial location of the cryoprobes is the studied parameter. The analysis is focused on a 2D domain, which represents the worst case scenario. It follows that the unfrozen region size around the urethral warmer in the real 3D domain is expected to

be not less than the region size identified in the current study. It was shown that steady state is likely to be reached in the region bounded by the cryoprobes, and therefore the analysis was focused on the steady state. Steady state represents a worst case scenario in the time domain.

The steady state analysis revealed a major effect of the heat exchanger wall thickness on the ability to warm the surrounding tissues, i.e. the urethra wall. For a heat exchanger wall thickness of 0.5 mm, it was shown that the cryoprobes must be localized at least 11 mm from the center of the heat exchanger, in order to heat the outer surface of the warmer above -45°C. Similarly, the cryoprobes must be localized at least 17 mm from the center of the heat exchanger in order to heat the outer surface of the warmer above -22°C, where the latter temperature is the assumed lower boundary for phase transition temperature range. Either way, the heating effect of the heat exchanger as a warmer is estimated as less than 1 mm when the cryoprobes are located at a radius of up to 20 mm. A radius of 20 mm can be considered as extremely large radius for cryoprobe localization in a typical prostate cryoprocedure.

It was found that the heating effect of the heat exchanger is not linearly dependent on its wall thickness. It was further found that an unrealistically thin wall thickness must be chosen in order to ensure an outer wall temperature above 0°C, for the entire applicable range of the cryoprobe localization radius.

It is estimated that, as a urethral warmer, the heat exchanger may fail to protect against freezing in a significant number of prostate cases. This conclusion is driven by bioheat transfer considerations. However, the existence of clinical reports is acknowledged, which suggest that the heat exchanger improves, in many cases, the outcome of cryosurgery in terms of long term complications. As a result of the current study, it is suggested that a correlation be sought between the layout of the cryoprobes around the urethra, and the long term follow up.

The cryoheater is expected to prevent freezing in a larger region than the heat exchanger. The unfrozen region thickness around the cryoheater is linearly dependent on the distance between the cryoprobes and the cryoheater.

REFERENCES

1. Altman PL & Dittmer DS, *Respiration and Circulation*, Federation of American Societies for Experimental Biology (Data Handbook), Bethesda, MD, 1971.
2. Chang Z, Finkelstein JJ, Ma H, & Baust J (1994) *Biomed Ins. & Tech* **28**, 383-390
3. Charny CK (1992) in *Advances in Heat Transfer* (eds) JP Hartnett, TF Irvine, & YI Cho, Academic Press, pp 19-156
4. Chato JC (1985) in *Heat Transfer in Biology and Medicine* (eds) A Shitzer, RC Eberhart, NY:Plenum Press pp 413-418
5. Chen MM & Holmes KR (1980) *Ann NY Acad Sci* **335**, 137-146
6. Cohen TK, Miller RJ, & Shumarz BA (1995) *Urology* **45**, 861-4
7. Cooper IS & Lee A (1961) *J Nerve Mental Dis* **133**, 259-263
8. Diller KR (1992) in *Advances in Heat Transfer* (eds) JP Hartnett, TF Irvine, & YI Cho, Academic Press, pp 157-358
9. Eberhart RC (1985) in *Heat Transfer in Biology and Medicine* (eds) A Shitzer, RC Eberhart, NY:Plenum Press. pp 261-324

10. Gage AA & Baust J (1998) *Cryobiology* **37**(3), 171-186
11. Klinger HG (1974) *General Theory Bull Math Biol* **36**, 403-418
12. Onik G et al (1985) AJR Am *J Roentgenol* **144**(5), 1043-7
13. Onik G et al (1988) *Radiology* **168**(3), 629-631
14. Onik GM et al (1993) *Cancer* **72**(4), 1291-1299,
15. Pennes HH (1948) *J App Phys* **1**, 93-122.
16. Rabin Y et al (1996) *Cryobiology* **33**, 93-105
17. Rabin Y & Shitzer A (1998) *ASME J Biomech Eng* **120**(1), 32-37.
18. Rabin Y, Julian TB, & Wolmark N (1999) US Patent No. 5,899,897
19. Rabin Y, Cryosurgery Workshop Series, Allegheny General Hospital, 2000-2002.
20. Rabin Y (2000) *CryoLetters* **21**, 163-170
21. Rabin Y & Stahovich TF (2002) *Phys Med Biol* Submitted
22. Rubinsky B et al (1993) *Cryobiology* **30**, 191-9
23. Weinbaum S & Jiji LM (1985) *ASME J Biomech Eng* **107**, 131-136
24. Wulff W (1974) *IEEE Trans Biomed Eng* BME-21, pp. 494.